

Supergiant Fast X-ray Transients in outburst: new *Swift* observations of XTE J1739–302, IGR J17544–2619 and IGR J08408–4503

L. Sidoli,^{1*} P. Romano,² L. Ducci,^{1,3} A. Paizis,¹ G. Cusumano,² V. Mangano,² H. A. Krimm,^{4,5} S. Vercellone,² D. N. Burrows,⁶ J. A. Kennea⁶ and N. Gehrels⁵

¹INAF, Istituto di Astrofisica Spaziale e Fisica Cosmica, Via E. Bassini 15, I-20133 Milano, Italy

²INAF, Istituto di Astrofisica Spaziale e Fisica Cosmica, Via U. La Malfa 153, I-90146 Palermo, Italy

³Dipartimento di Fisica e Matematica, Università dell'Insubria, Via Valleggio 11, I-22100 Como, Italy

⁴Universities Space Research Association, Columbia, MD 21044-34342, USA

⁵NASA/Goddard Space Flight Center, Greenbelt, MD 20771, USA

⁶Department of Astronomy and Astrophysics, Pennsylvania State University, University Park, PA 16802, USA

Accepted 2009 May 14. Received 2009 May 14; in original form 2009 March 6

ABSTRACT

We report on new X-ray outbursts observed with *Swift* from three Supergiant Fast X-ray Transients (SFXTs): XTE J1739–302, IGR J17544–2619 and IGR J08408–4503. XTE J1739–302 underwent a new outburst on 2008 August 13, IGR J17544–2619 on 2008 September 4 and IGR J08408–4503 on 2008 September 21. While the XTE J1739–302 and IGR J08408–4503 bright emission triggered the *Swift*/Burst Alert Telescope, IGR J17544–2619 did not, thus we could perform a spectral investigation only of the spectrum below 10 keV. The broad-band spectra from XTE J1739–302 and IGR J08408–4503 were compatible with the X-ray spectral shape displayed during the previous flares. A variable absorbing column density during the flare was observed in XTE J1739–302 for the first time. The broad-band spectrum of IGR J08408–4503 requires the presence of two distinct photon populations, a cold one (~ 0.3 keV) most likely from a thermal halo around the neutron star and a hotter one (1.4–1.8 keV) from the accreting column. The outburst from XTE J1739–302 could be monitored with a very good sampling, thus revealing a shape which can be explained with a second wind component in this SFXT, in analogy to what we have suggested in the periodic SFXT IGR J11215–5952. The outburst recurrence time-scale in IGR J17544–2619 during our monitoring campaign with *Swift* suggests a long orbital period of ~ 150 d (in a highly eccentric orbit), compatible with what previously observed with *INTEGRAL*.

Key words: X-rays: binaries – X-rays: individual: XTE J1739–302 – X-rays: individual: IGR J17544–2619 – X-rays: individual: IGR J08408–4503.

1 INTRODUCTION

The discovery of a new class of Galactic bright X-ray transients, composed of a compact object and an OB supergiant companion, the so-called Supergiant Fast X-ray Transients (SFXTs), is one of the most intriguing results obtained by the *INTEGRAL* satellite (Sguera et al. 2005, Negueruela et al. 2006). Since its launch in 2002 October, the Galactic plane monitoring performed with *INTEGRAL*/IBIS led to the discovery of several new sources (Bird et al. 2007), some of which were characterized by short flares reaching 10^{36} – 10^{37} erg s^{–1}, and later optically associated with blue supergiant stars (e.g. Masetti et al. 2006b). A couple of members of the class were discovered years before 2002, with other satellites, and later re-discovered with *INTEGRAL* and firmly classified as SFXTs: XTE J1739–302

(Smith et al. 1998), now considered the prototype of the class, and the X-ray pulsar AX J1841.0–0536 (Bamba et al. 2001). SFXTs display a broad-band spectral shape similar to that of accreting X-ray pulsars (Walter et al. 2006), and a high dynamic range in X-rays (up to four or five orders of magnitude) down to a quiescent luminosity at $\sim 10^{32}$ erg s^{–1} (in't Zand 2005). Although X-ray pulsations have not been discovered, to date, in all the members of the class, the spectral similarity with the accreting X-ray pulsars suggests that all, or at least most of them, host neutron stars. Their peculiar transient behaviour is still waiting for a convincing theoretical explanation, although all the physical mechanisms proposed to date are mainly related to the structure of the supergiant wind and/or to the properties of the accreting neutron star (see Sidoli 2009 and references therein for a recent review).

The first systematic monitoring of the X-ray activity of SFXTs has been performed with *Swift*, during a campaign (still in progress) which started in 2007 October, with the main aim of studying the

*E-mail: sidoli@lambrate.inaf.it

long-term properties of a sample of SFXTs: XTE J1739–302/IGR J17391–3021, IGR J17544–2619, IGR J16479–4514 and AX J1841.0–0536/IGR J18410–0535 (Sidoli et al. 2008b, hereafter Paper I).

One of the important results of these *Swift* observations is the discovery that SFXTs do not spend most of the time in quiescence, as previously thought, but in an intermediate level of emission at around 10^{33} – 10^{34} erg s^{−1}, displaying a hard X-ray spectrum and a frequent low-intensity flaring activity, with a dynamic range of more than one order of magnitude (Paper I).

During the *Swift* monitoring, about 1–2 bright outbursts per year per source have been caught (IGR J16479–4514, Romano et al. 2008c, hereafter Paper II; IGR J17544–2619 and XTE J1739–302, Sidoli et al. 2009, hereafter Paper III), leading to the study of the first broad-band spectrum from these sources, observed simultaneously from 0.3 to 60 keV. The results of a *Swift* monitoring of a multiflaring X-ray activity in 2008 July from the fifth SFXT, IGR J08408–4503, have been reported by Romano et al. (2009a).

In this paper, we report on the latest three outbursts caught by *Swift* from three SFXTs, already announced to the scientific community: XTE J1739–302 (2008 August 13; Romano et al. 2008b), IGR J17544–2619 (2008 September 4; Romano et al. 2008a), IGR J08408–4503 (2008 September 21; Mangano et al. 2008).

1.1 Previous observations of the three SFXTs

XTE J1739–302 was discovered by *RXTE* in 1997 August (Smith et al. 1998), reaching a peak flux of 3.6×10^{-9} erg cm^{−2} s^{−1} (2–25 keV). The optical counterpart is an O8 Iab(f) star (Negueruela et al. 2006) located at 2.7 kpc (Rahoui et al. 2008). *ASCA* observations (Sakano et al. 2002) allowed a constraint on the quiescent emission at a level of $< 1.1 \times 10^{-12}$ erg cm^{−2} s^{−1}. The source showed bright outbursts, reaching 300 mCrab, observed with *IBIS/ISGRI* in 2003 and 2004 March (Sguera et al. 2006). Other flares observed with *INTEGRAL* have been reported by Walter & Zurita Heras (2007) and Blay et al. (2008). More recently, it triggered the *Swift* Burst Alert Telescope (BAT) on 2008 April 8, when a bright flare was caught, reaching an X-ray luminosity of $\sim 3 \times 10^{36}$ erg s^{−1} (0.5–100 keV; Paper III). Since 2007 October, the source has been monitored with *Swift*/XRT approximately two to three times a week, showing a high variability in its flux even outside outbursts (Paper I).

IGR J17544–2619 was discovered with *INTEGRAL* on 2003 September 17 during a short flare reaching 160 mCrab (18–25 keV; Sunyaev et al. 2003). A *Chandra* observation performed in 2004 caught both the quiescence level and the onset of an outburst (in’t Zand 2005), translating into a dynamic range as large as 10^4 . The optical counterpart is an O9Ib star (Pellizza, Chaty & Negueruela 2006) located at 3.6 kpc (Rahoui et al. 2008). Several more bright flares have been observed with *INTEGRAL* in 2003–2005 (Grebenev, Lutovinov & Sunyaev 2003; Grebenev et al. 2004; Sguera et al. 2006; Kuulkers et al. 2007; Walter & Zurita Heras 2007; Ducci et al. 2008). Two outbursts were detected with the *Swift* satellite, on 2007 November 8 (Krimm et al. 2007) and 2008 March 31 (Sidoli et al. 2008a), 144 d apart. Fainter activity at a level of 30–40 mCrab (20–60 keV) from IGR J17544–2619 was also observed on 2007 September 21, with *IBIS/ISGRI* on-board *INTEGRAL* (Kuulkers et al. 2007). IGR J17544–2619 is one of the four SFXTs we have been monitoring with *Swift*/XRT since 2007 October (Paper I).

IGR J08408–4503 was discovered on 2006 May 15, when a bright flare reaching a peak flux of 250 mCrab in the 20–40 keV energy band was caught by *INTEGRAL* (Götz et al. 2006). Analysis

of archival *INTEGRAL* observations of the source field showed that IGR J08408–4503 was previously active on 2003 July 1 (Mereghetti et al. 2006). A refined position with *Swift*/XRT (Kennea & Campana 2006) allowed to associate the source with a O8.5Ib(f) supergiant star, HD 74194, at a distance of about 3 kpc (Masetti et al. 2006a). Three additional flares observed with *INTEGRAL* and *Swift* were studied by Götz et al. (2007). A new outburst from IGR J08408–4503 was caught on 2008 July 5 by *Swift*/BAT and then followed up at softer energies with *Swift*/XRT (Romano et al. 2009a). In that occasion, the source displayed a multiple flaring activity (the XRT light curve showed three bright flares in excess of 10 s^{−1}). The properties of the flares and of the times of the outbursts suggested an orbital period of ~ 35 d (Romano et al. 2009a).

2 OBSERVATIONS AND DATA REDUCTION

As a response to a first BAT trigger from XTE J1739–302 on 2008 August 13 at 23:49:17 UT (image trigger 319963), *Swift* executed an immediate slew and was on target in ~ 390 s; a second trigger (319964) occurred while XTE J1739–302 was in the XRT field of view on 2008 August 14 at 00:12:53 UT. The bright flare of IGR J17544–2619 was instead discovered as part of the yearly monitoring with *Swift*/XRT, starting on 2008 September 04 at about 00:19:00 UT. The *Swift*/BAT did not trigger on it. IGR J08408–4503 triggered the BAT on 2008 August 21 at 07:55:08 UT (image trigger 325461). *Swift* slewed immediately and the narrow field instruments were on target in ~ 147 s.

Table 1 reports the log of the *Swift* observations of the outbursts used for this work. The XRT data were processed with standard procedures (XRTPIPELINE v0.12.1), filtering and screening criteria by using FTOOLS in the HEASOFT package (v.6.6.1). We considered both windowed timing (WT) and photon counting (PC) data, and selected event grades 0–2 and 0–12, respectively (Burrows et al. 2005). When appropriate, we corrected for pile-up by determining the size of the point spread function (PSF) core affected by comparing the observed and nominal PSF (Vaughan et al. 2006), and excluding all the events that fell within that region from the analysis. Background events were extracted in source-free annular regions, centred on the source. Ancillary response files were generated with XRTMKARF, and they account for different extraction regions, vignetting and PSF corrections. We used the latest spectral redistribution matrices (v011) in CALDB.

The BAT data were collected in event mode for several hundred seconds after the triggers of XTE J1739–302 and IGR J08408–4503, as detailed below, while IGR J17544–2619 was not detected. The BAT data were analysed using the standard BAT analysis software distributed within FTOOLS. The BAT mask-weighted spectra were extracted over the time intervals simultaneous with XRT data when possible, and response matrices were generated with BATDRMGEN. For our spectral fitting (XSPEC v11.3.2), we applied an energy-dependent systematic error.

All quoted uncertainties are given at 90 per cent confidence level for one interesting parameter unless otherwise stated. The spectral indices are parametrized as $F_\nu \propto \nu^{-\alpha}$, where F_ν (erg cm^{−2} s^{−1} Hz^{−1}) is the flux density as a function of frequency ν ; we adopt $\Gamma = \alpha + 1$ as the photon index, $N(E) \propto E^{-\Gamma}$ (ph cm^{−2} s^{−1} keV^{−1}). Times in the light curves and the text are referred to their respective BAT triggers with the exception of IGR J17544–2619 which did not trigger the BAT, thus the start time was set at the beginning of the observation.

Table 1. Observation log.

Source	Sequence	Instrument /mode	Start time (UT) (yyyy-mm-dd hh:mm:ss)	End time (UT) (yyyy-mm-dd hh:mm:ss)	Exposure (s)
XTE J1739–302	00319963000	BAT/event	2008-08-13 23:47:14	2008-08-14 00:05:22	1088
	00319963000	XRT/WT	2008-08-13 23:55:55	2008-08-14 00:29:09	1688
	00319963000	XRT/PC	2008-08-14 00:03:19	2008-08-14 00:04:34	75
	00319964000	BAT/event	2008-08-14 00:08:56	2008-08-14 00:28:58	728
	00030987070	XRT/WT	2008-08-14 01:23:10	2008-08-14 13:03:50	1207
	00030987070	XRT/PC	2008-08-14 04:36:11	2008-08-14 13:17:16	10714
	00030987071	XRT/PC	2008-08-15 00:00:34	2008-08-15 00:16:57	983
	00030987072	XRT/PC	2008-08-16 03:21:09	2008-08-16 05:08:57	1379
	00030987073	BAT/PC	2008-08-17 01:44:09	2008-08-17 02:01:57	1068
	00030987074	XRT/PC	2008-08-18 13:04:08	2008-08-18 13:21:56	1068
	00030987075	XRT/PC	2008-08-19 13:09:42	2008-08-19 13:27:58	1095
	00030987076	XRT/PC	2008-08-20 05:14:06	2008-08-20 05:31:56	1071
	00030987077	XRT/PC	2008-08-21 00:30:30	2008-08-21 15:08:55	1173
	00030987078	XRT/PC	2008-08-22 00:36:19	2008-08-22 02:21:55	1093
	00030987079	XRT/PC	2008-08-23 03:55:11	2008-08-23 05:41:56	1229
	00030987080	XRT/PC	2008-08-24 21:44:19	2008-08-24 23:31:57	1332
	00030987081	XRT/PC	2008-08-25 21:50:21	2008-08-25 23:35:56	1274
	IGR J08408–4503	00325461000	BAT/event	2008-09-21 07:54:11	2008-09-21 09:16:38
00325461000		XRT/WT	2008-09-21 08:03:54	2008-09-21 14:05:06	1159
00325461000		XRT/PC	2008-09-21 09:16:31	2008-09-21 14:24:59	4116
00030707013		XRT/PC	2008-09-23 15:53:39	2008-09-23 17:36:57	1109
00030707014		XRT/PC	2008-09-25 18:15:07	2008-09-25 19:57:54	1094
00030707015		XRT/PC	2008-09-26 18:10:01	2008-09-26 18:26:37	995
00030707016		XRT/PC	2008-09-27 16:39:46	2008-09-27 18:19:57	216
00030707017		XRT/PC	2008-09-28 16:56:30	2008-09-28 17:01:26	295
IGR J17544–2619	00035056061	XRT/WT	2008-09-04 00:12:40	2008-09-04 00:25:03	217
	00035056061	XRT/PC	2008-09-04 00:12:45	2008-09-04 00:26:55	632

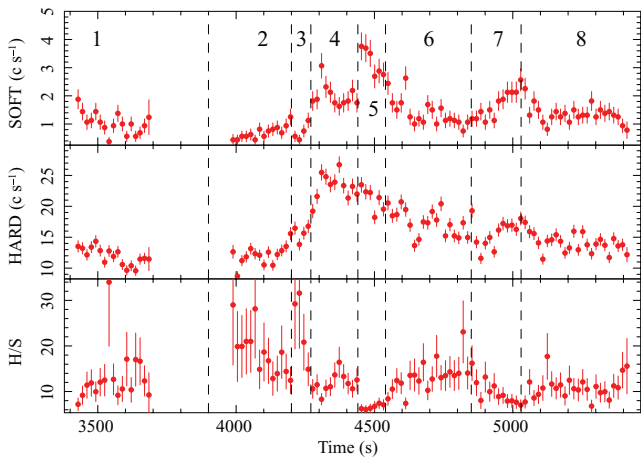


Figure 1. *Swift*/XRT (WT data) light curves of XTE J1739–302 in two energy ranges, 0.3–2 keV (soft, upper panel) and 2–10 keV (hard, middle panel), together with their hardness ratio (lower panel). Vertical dashed lines mark the eight spectra selected for the time-resolved spectroscopy.

3 ANALYSIS AND RESULTS

3.1 XTE J1739–302

The complete light curve of the bright flaring of XTE J1739–302 as observed with *Swift*/XRT on 2008 August 13 is reported in Fig. 9(c), while the first part (~ 2000 s) of the observation (WT data, observation 00319963000) is expanded in Fig. 1, where a soft (below 2 keV) and a hard (above 2 keV) light curve are reported, together with

their hardness ratio. Since the source hardness appears to be variable, we performed a time-resolved spectroscopy extracting eight XRT/WT spectra as shown in Fig. 1. These spectra could be adequately fitted both with an absorbed power-law model and with an absorbed single blackbody (BB; see Table 2 for the results, spectra from WT 1 to WT 8). There is a clear time variability of the absorbing column density (by a factor of ~ 3), whereas the spectral shape (photon index, Γ , or the BB temperature, kT_{bb}) remains constant, within the uncertainties (see Fig. 2). In particular, spectra WT 3 and WT 5 are the hardest and the softest ones, respectively, thus demonstrating that the hardness ratio variability in Fig. 1 is due to a variable absorption into the line of sight. As final tests, we fixed the photon index $\Gamma = 1.15$ (average value) and then re-fitted the eight spectra. This still resulted in a variable absorbing column density. We then fixed the absorbing column density to a mean value of $5 \times 10^{22} \text{ cm}^{-2}$ and refitted the spectra. Those spectra where the absorption was previously found to be very different from this mean value resulted in unacceptable fits.

Fig. 3 shows the comparison between the time-resolved spectroscopy of the XRT/WT data (Table 2) of the 2008 August outburst and two more spectral analyses: the out-of-outburst emission (Paper I) and the spectroscopy of a previous flare from XTE J1739–302 (Paper III). There is no evidence for a spectral change with the source flux, or for a correlation of the absorbing column density with the source flux. The absorption is higher during the rising phase of the bright flare.

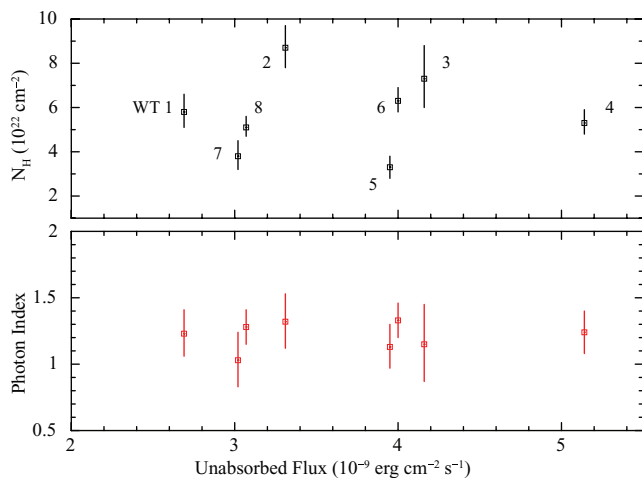
A high-energy spectrum (BAT) was also available, but only simultaneously to the XRT/WT spectrum n. 1. A joint fit of XRT/WT and BAT spectra was performed including constant factors to allow for normalization uncertainties between the two instruments

Table 2. Time-resolved spectroscopy of XTE J1739–302 (XRT data).

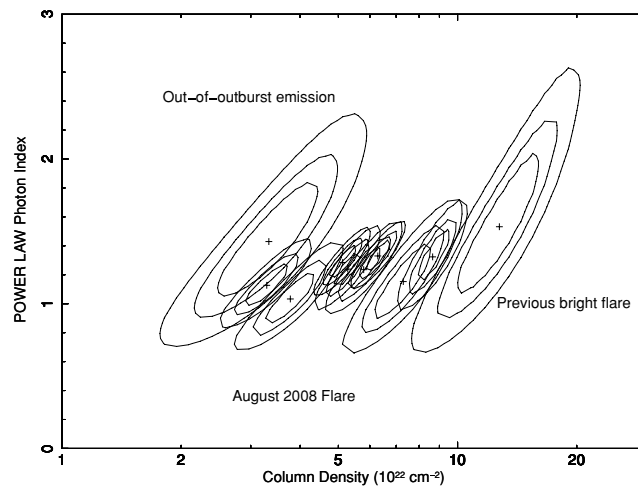
Spectrum	Time (s since trigger)	Model	N_{H} (10^{22} cm $^{-2}$)	Γ	kT_{bb} (keV)	Flux ^a	R_{bb} (km) ^b	χ^2_{ν} /d.o.f.
WT 1	397–656	Pow	$5.8^{+0.8}_{-0.7}$	$1.23^{+0.18}_{-0.17}$		2.69		1.191/139
		BB	$3.1^{+0.5}_{-0.4}$		$1.88^{+0.12}_{-0.11}$		$1.1^{+0.1}_{-0.1}$	1.044/139
WT 2	961–1170	Pow	$8.7^{+1.0}_{-0.9}$	$1.32^{+0.21}_{-0.20}$		3.31		1.038/112
		BB	$5.4^{+0.7}_{-0.6}$		$1.93^{+0.16}_{-0.14}$		$1.2^{+0.2}_{-0.1}$	1.080/112
WT 3	1170–1255	Pow	$7.3^{+1.5}_{-1.3}$	$1.15^{+0.30}_{-0.28}$		4.16		0.873/66
		BB	$4.4^{+0.9}_{-0.8}$		$1.98^{+0.23}_{-0.19}$		$1.3^{+0.3}_{-0.2}$	0.809/66
WT 4	1255–1407	Pow	$5.3^{+0.6}_{-0.5}$	$1.24^{+0.16}_{-0.16}$		5.14		0.961/159
		BB	$2.8^{+0.4}_{-0.3}$		$1.82^{+0.11}_{-0.10}$		$1.7^{+0.2}_{-0.1}$	0.910/159
WT 5	1410–1520	Pow	$3.3^{+0.5}_{-0.5}$	$1.13^{+0.17}_{-0.16}$		3.95		1.074/114
		BB	$1.4^{+0.3}_{-0.2}$		$1.80^{+0.12}_{-0.11}$		$1.5^{+0.2}_{-0.1}$	0.846/114
WT 6	1522–1876	Pow	$6.3^{+0.6}_{-0.5}$	$1.33^{+0.13}_{-0.13}$		4.00		1.241/243
		BB	$3.4^{+0.3}_{-0.3}$		$1.83^{+0.08}_{-0.08}$		$1.4^{+0.1}_{-0.1}$	1.047/243
WT 7	1877–2005	Pow	$3.8^{+0.7}_{-0.6}$	$1.03^{+0.21}_{-0.20}$		3.02		1.345/98
		BB	$1.8^{+0.4}_{-0.3}$		$1.90^{+0.16}_{-0.14}$		$1.2^{+0.2}_{-0.1}$	1.227/98
WT 8	2006–2390	Pow	$5.1^{+0.5}_{-0.4}$	$1.28^{+0.13}_{-0.13}$		3.07		1.083/229
		BB	$2.6^{+0.3}_{-0.3}$		$1.82^{+0.09}_{-0.08}$		$1.3^{+0.1}_{-0.1}$	0.969/229
WT 9 ^c	5631–47671	Pow	$3.6^{+0.4}_{-0.3}$	$1.1^{+0.1}_{-0.1}$		1.02		1.396/259
		BB	$1.5^{+0.2}_{-0.2}$		$1.89^{+0.08}_{-0.07}$		$0.72^{+0.05}_{-0.04}$	1.128/259
PC 1 ^c	17212–48475	Pow	$3.0^{+0.4}_{-0.4}$	$1.26^{+0.17}_{-0.16}$		0.23		1.095/113
		BB	$1.3^{+0.2}_{-0.2}$		$1.64^{+0.10}_{-0.09}$		$0.43^{+0.04}_{-0.03}$	1.082/113

^aUnabsorbed 1–10 keV flux in units of 10^{-9} erg cm $^{-2}$ s $^{-1}$.

^bAssuming a distance of 2.7 kpc.

^cObservation 00030987070.

Figure 2. *Swift*/XRT (WT data) time-resolved spectroscopy of XTE J1739–302: spectral results of the absorbed power-law fit (reported in Table 2). Numbers mark the eight WT spectra, as shown in Table 2.

(always constrained to be within their usual ranges). A single power law is unable to describe the broad-band spectrum. We then tried models usually adopted to describe the X-ray emission from accreting pulsars, resulting in the spectral parameters listed in Table 3: a cut-off power law [$E^{-\Gamma} e^{(-E/E_{\text{cut}})}$] and two kinds of Comptonization models. The best deconvolution of the broad-band spectrum has been obtained with these latter models: a Comptonization of seed photons (with a temperature kT_0) in a hot plasma (with elec-


Figure 3. *Swift*/XRT (WT data) time-resolved spectroscopy (eight spectra reported in Table 2) of XTE J1739–302 during the new outburst observed on 2008 August 13 (absorbed power law) compared with the spectral parameters derived during the previous bright flare observed with *Swift* (discussed in Paper III; large contours on the right). The power-law parameters of the total spectrum of the out-of-outburst emission (Paper I) are also shown (large contours on the left). 68, 90 and 99 per cent confidence level contours are shown.

tron temperature kT_e) as described by *COMP*TT in *XSPEC* (Titarchuk 1994) or by *BMC* (Titarchuk, Mastichiadis & Kylafis 1996).

The *BMC* model is the sum of a *BB* plus its Comptonization, the latter obtained as a consistent convolution of the *BB* itself with Green's function of the Compton corona. The *BMC* model is not

Table 3. Spectral fits of simultaneous XRT and BAT data of XTE J1739–302.

Model	Parameters					
CUT-OFFPL	N_{H}^{a}	Γ	$E_{\text{cut}}^{\text{b}}$	Flux ^c	$\chi^2_{\nu}/\text{d.o.f.}$	
	$5.5^{+0.8}_{-0.8}$	$0.87^{+0.27}_{-0.28}$	15^{+6}_{-4}	6.6	1.166/161	
BMC	N_{H}^{a}	$kT_{\text{BB}}^{\text{b,d}}$	α^{d}	$\log A^{\text{d}}$	Flux ^c	$\chi^2_{\nu}/\text{d.o.f.}$
	$3.4^{+0.6}_{-0.5}$	$1.6^{+0.2}_{-0.3}$	$1.3^{+0.4}_{-0.4}$	$0.5^{+7.5}_{-0.6}$	4.9	1.080/160
COMP TT ^e	N_{H}^{a}	kT_0^{b}	kT_e^{b}	τ	Flux ^c	$\chi^2_{\nu}/\text{d.o.f.}$
	$2.8^{+0.6}_{-0.5}$	$1.35^{+0.12}_{-0.17}$	>9	$4.3^{+3.6}_{-4.0}$	4.6	1.061/160

^aAbsorbing column density is in units of 10^{22} cm^{-2} .

^bHigh-energy cut-off (E_{cut}), electron temperature (kT_e), seed photons temperature (kT_0) and the BB colour temperature kT_{BB} are all in units of keV.

^cUnabsorbed 0.1–100 keV flux is in units of $10^{-9} \text{ erg cm}^{-2} \text{ s}^{-1}$.

^d kT_{BB} is the BB colour temperature of the seed photons, α is the spectral index and $\log A$ is the illumination parameter (see Section 3.1 for details).

^eAssuming a spherical geometry.

limited to the thermal Comptonization case (as e.g. COMP TT) and accounts also for dynamical (bulk) Comptonization due to the converging flow. Similar to the ordinary BBODY XSPEC model, the normalization of BMC is the ratio of the source luminosity to the square of the distance (in units of 10 kpc). The free parameters of the BMC model (apart from the normalization) are the blackbody (BB) colour temperature, kT_{BB} , the spectral index, α , and the logarithm of the illuminating factor A , $\log A$. The parameter α indicates the overall Comptonization efficiency related to an observable quantity in the photon spectrum of the data. The lower α , the higher the efficiency that is the higher the energy transfer from the hot electrons to the soft seed photons. The $\log A$ parameter is an indication of the fraction of the up-scattered BB photons with respect to the BB seed photons directly visible. In the extreme cases, the seed photons can be completely embedded in the Comptonizing cloud (none directly visible, $A \gg 1$, e.g. $\log A = 8$) or there is no coverage by the Compton cloud ($A \ll 1$, e.g. $\log A = -8$), and we directly observe the seed photon spectrum (equivalent to a simple BB, with no Comptonization).

The XTE J1739–302 broad-band spectrum fitted with the COMP TT model is shown in Fig. 4. The estimated X-ray luminosity during the flare is $3.8 \times 10^{36} \text{ erg s}^{-1}$ (0.1–100 keV) at a source distance of 2.7 kpc.

As can be seen in Table 3, the parameters describing the properties of the Comptonizing corona (be they the temperature and optical depth in COMP TT or the illumination parameter $\log A$ in BMC) are not constrained. This is expected, given the poor statistics of the high-energy part of the spectrum. Nevertheless, the applied models do give a first-order description of the physical processes involved in this system (see Section 4).

3.2 IGR J17544–2619

A new bright flare from IGR J17544–2619 was caught on 2008 September 4 with *Swift*, and it was preceded by intense activity in the previous few days observed during the *INTEGRAL* Galactic bulge monitoring program (Romano et al. 2008a), reaching about 50 mCrab (18–40 keV) on 2008 August 30. The flare was caught by *Swift*/XRT, only thanks to the on-going monitoring campaign just targeted on the source, while *Swift*/BAT did not trigger on it. The XRT light curve (Fig. 5) shows a peak exceeding 20 s^{-1} , brighter than the previous one observed with *Swift* on March 31, at 20:53:27 UT (Paper III).

The total PC spectrum resulted in an exposure time of 632 s and a source net count rate of $0.67 \pm 0.03 \text{ s}^{-1}$, while the WT data,

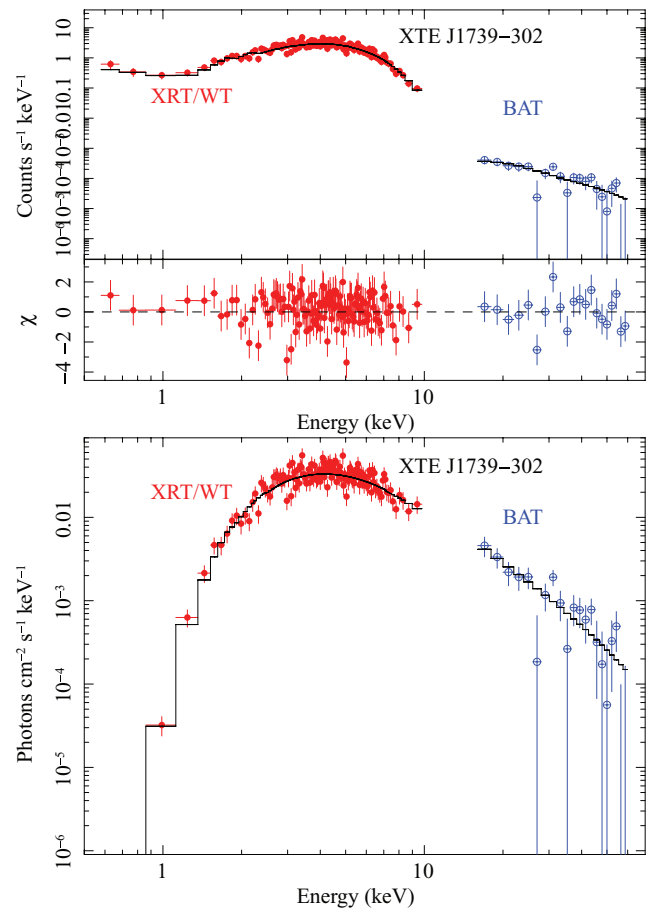


Figure 4. XTE J1739–302 broad-band spectrum (XRT/WT together with BAT data) fitted with a Comptonization model (COMP TT in XSPEC).

extracted with a net exposure of 217 s, resulted in an average count rate of $8.2 \pm 0.2 \text{ s}^{-1}$. Fitting the two spectra separately with simple models (an absorbed power law or a BB) resulted in the parameters listed in Table 4. A BB is a better fit to the WT data than a single power law, which produces systematic positive residuals around 1 keV. The resulting BB radius at an assumed source distance of 3.6 kpc is $R_{\text{bb}} = 1.35^{+0.15}_{-0.12} \text{ km}$. More complex models are not required by the data. We also fit together PC and WT spectra, adopting free normalization constant factors between the two spectra. The best fit

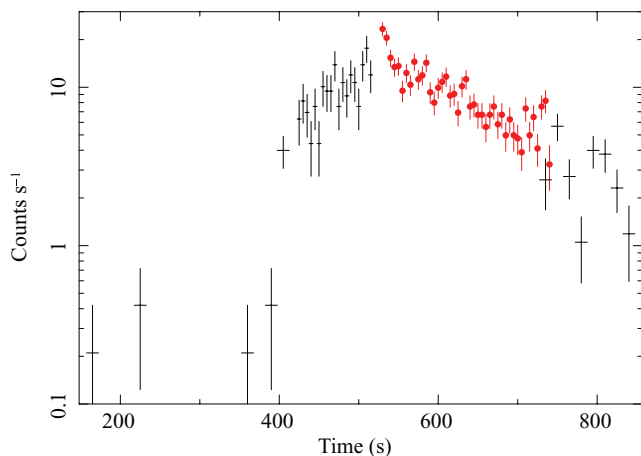


Figure 5. *Swift*/XRT light curve of IGR J17544–2619 during the outburst observed on 2008 September 4. Crosses mark the WT spectrum and circles refer to PC data.

obtained with a BB model of the joint PC plus WT data is reported in Fig. 6.

3.3 IGR J08408–4503

The IGR J08408–4503 *Swift*/XRT light curve during the new outburst detected on 2008 September 21 is reported in Fig. 7 in two energy ranges, together with their hardness ratio. Since the hardness ratio was quite constant along the XRT/WT observation, we extracted a total spectrum. It resulted in a net exposure time of 1159 s with an average count rate of $28.3 \pm 0.2 \text{ s}^{-1}$. The fit to the 0.7–10 keV WT spectrum with an absorbed power-law model is unacceptable ($\chi^2_{\nu} = 1.309$ for 630 d.o.f.). A significantly better fit can be obtained either with a cut-off power law ($\chi^2_{\nu} = 1.187$ for 629 d.o.f.) or with a power-law model together with a BB ($\chi^2_{\nu} = 1.116$ for 628 d.o.f.). We note that an absorbed BB model is the worst fit to the WT data, resulting in a reduced $\chi^2_{\nu} > 3.6$. The peak flux of $\sim 2.5 \times 10^{-9} \text{ erg cm}^{-2} \text{ s}^{-1}$ translates into an X-ray luminosity of $2.5 \times 10^{36} \text{ erg s}^{-1}$ (at 3 kpc).

The spectral parameters resulting from these fits are reported in Table 5. A second total spectrum from the fainter emission observed in PC mode has been also investigated, yielding a spectrum with a net exposure of 4100 s, and a fainter rate of $0.26 \pm 0.08 \text{ s}^{-1}$. A fit with a single absorbed power law results into a softer spectrum than the brighter emission observed in WT mode (see Table 5 for the PC spectral results).

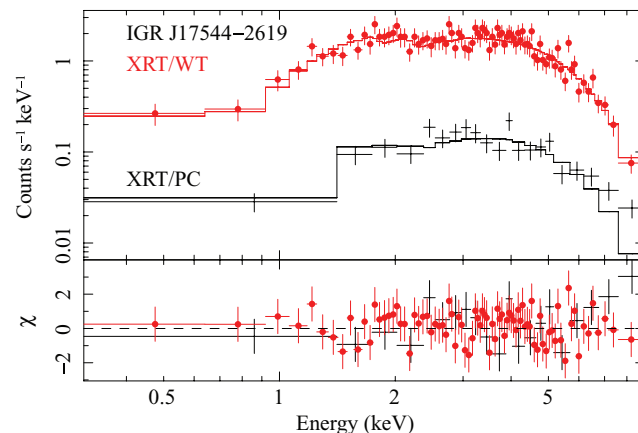


Figure 6. IGR J17544–2619 spectra (PC plus WT data) fitted with an absorbed BB (see Table 4 for the parameters), together with the residuals in units of standard deviations. Crosses mark the WT spectrum and circles refer to PC data (same as Fig. 5).

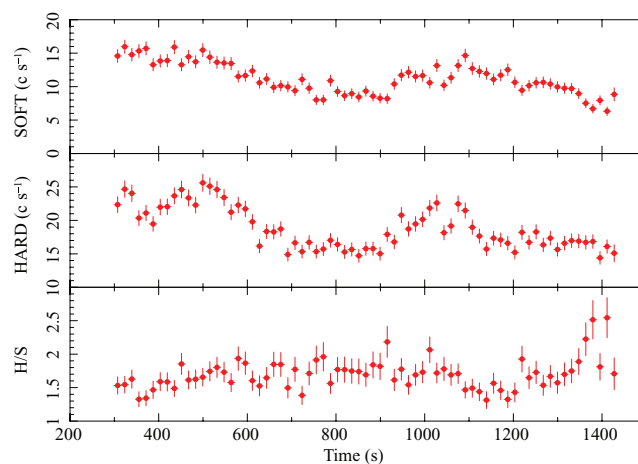


Figure 7. *Swift*/XRT light curves (WT data) of IGR J08408–4503 during the 2008 September 21 outburst (time is in seconds since the BAT trigger). The bin time is 16 s. The soft and hard energy ranges are below and above 2 keV, respectively. The lower panel shows their hardness ratio.

A BAT spectrum could also be extracted at the beginning of the observation, with a net exposure time of 200 s and a source count rate of $35.8 \pm 0.5 \text{ s}^{-1}$ (14–60 keV). Fitting the BAT and XRT simultaneous spectra with a single power law resulted in an unacceptable reduced χ^2_{ν} of 2.38 (293 d.o.f.). A very good

Table 4. IGR J17544–2619 spectral fits of XRT data.

Spectrum	Model	N_{H} (10^{22} cm^{-2})	Γ	kT_{bb} (keV)	Flux ^a	R_{bb} (km) ^b	$\chi^2_{\nu}/\text{d.o.f.}$
Total WT	Pow	$1.8^{+0.4}_{-0.3}$	$1.28^{+0.18}_{-0.19}$		0.97		1.170/82
	BB	$0.52^{+0.17}_{-0.14}$		$1.51^{+0.10}_{-0.09}$		$1.35^{+0.15}_{-0.12}$	0.808/82
Total PC	Pow	$1.3^{+0.8}_{-0.5}$	$0.76^{+0.40}_{-0.35}$		0.27		1.290/18
	BB	$0.42^{+0.38}_{-0.26}$		$1.87^{+0.40}_{-0.29}$		$0.51^{+0.17}_{-0.10}$	1.080/18
Joint fit WT + PC	Pow	$1.8^{+1.0}_{-0.9}$	$1.20^{+0.17}_{-0.16}$				1.227/102
	BB	$0.52^{+0.15}_{-0.13}$		$1.55^{+0.09}_{-0.09}$			0.979/102

^aUnabsorbed 1–10 keV flux in units of $10^{-9} \text{ erg cm}^{-2} \text{ s}^{-1}$.

^bAssuming a distance of 3.6 kpc.

Table 5. IGR J08408–4503 spectral fits of XRT data.

Spectrum	Time (s since trigger)	Model	N_{H} (10^{22} cm^{-2})	Γ	$kT_{\text{bb}}/E_{\text{cut}}$ (keV)	Flux ^a	R_{bb} (km) ^b	$\chi^2_{\nu}/\text{d.o.f.}$
Total WT	523–1653	Pow	$0.25^{+0.02}_{-0.02}$	$0.82^{+0.03}_{-0.03}$		2.7		1.309/630
		Pow+BB	$0.43^{+0.09}_{-0.09}$	$2.20^{+0.04}_{-0.04}$	$1.95^{+0.08}_{-0.08}$	2.5	$1.22^{+0.12}_{-0.12}$	1.116/628
		CUT-OFFPL	$0.11^{+0.03}_{-0.03}$	$0.22^{+0.12}_{-0.12}$	$6.6^{+1.5}_{-1.1}$	2.5		1.187/629
Total PC	4880–23388	Pow	$0.70^{+0.24}_{-0.19}$	$1.10^{+0.18}_{-0.16}$		0.056		1.126/50
		BB	<0.1		$1.44^{+0.09}_{-0.09}$	0.044	$0.31^{+0.04}_{-0.03}$	1.170/50

^aUnabsorbed 1–10 keV flux in units of $10^{-9} \text{ erg cm}^{-2} \text{ s}^{-1}$.

^bAssuming a distance of 3 kpc.

Table 6. Spectral fits of simultaneous XRT and BAT data of IGR J08408–4503. See Section 3.3 for the description of the adopted models.

Model	Parameters									
CUT-OFFPL	N_{H}^{a}	Γ	$E_{\text{cut}}^{\text{b}}$						Flux ^c	$\chi^2_{\nu}/\text{d.o.f.}$
	$0.10^{+0.04}_{-0.04}$	$0.50^{+0.08}_{-0.08}$	13^{+2}_{-2}						10	1.029/292
BMC*HIGHECUT+BB	N_{H}^{a}	$kT_{\text{BB}}^{\text{b,d}}$	α^{d}	$\log(A)^{\text{d}}$	$E_{\text{cut}}^{\text{b}}$	$E_{\text{fold}}^{\text{b}}$	$kT_{\text{BBbody}}^{\text{b}}$	$R_{\text{BBbody}}^{\text{e}}$	Flux ^c	$\chi^2_{\nu}/\text{d.o.f.}$
	$0.10^{+0.70}_{-0.05}$	$0.32^{+0.05}_{-0.06}$	$6^{+13}_{-5} \times 10^{-4}$	$3.3^{+0.5}_{-0.2}$	21^{+4}_{-7}	18^{+5}_{-4}	$1.85^{+0.16}_{-0.13}$	$1.2^{+0.2}_{-0.8}$	10	0.996/287
BMC*HIGHECUT+BB	N_{H}^{a}	$kT_{\text{BB}}^{\text{b,d}}$	α^{d}	$\log(A)^{\text{d}}$	$E_{\text{cut}}^{\text{b}}$	$E_{\text{fold}}^{\text{b}}$	$kT_{\text{BBbody}}^{\text{b}}$	$R_{\text{BBbody}}^{\text{e}}$	Flux ^c	$\chi^2_{\nu}/\text{d.o.f.}$
	$0.10^{+0.06}_{-0.03}$	$1.4^{+0.1}_{-0.1}$	$0.35^{+0.08}_{-0.06}$	$0.82^{+0.15}_{-0.14}$	21^{+5}_{-12}	22^{+8}_{-5}	$0.33^{+0.82}_{-0.04}$	12^{+4}_{-1}	10	0.988/287

^aAbsorbing column density is in units of 10^{22} cm^{-2} .

^bHigh-energy cut-off (E_{cut}), e-folding energy (E_{fold}) and BB temperatures are in units of keV.

^cUnabsorbed 0.1–100 keV flux is in units of $10^{-9} \text{ erg cm}^{-2} \text{ s}^{-1}$.

^d kT_{BB} is the BB colour temperature of the seed photons in the BMC model, α is the spectral index and $\log A$ is the illumination parameter.

^eThe radius of the BBODY model is in units of km at an assumed source distance of 3 kpc.

fit can be obtained with a cut-off power law (CUT-OFFPL in XSPEC; $\chi^2_{\nu} = 1.029$, for 292 d.o.f.), obtaining a hard spectrum with a photon index of 0.5, a cut-off at 13 keV, and a luminosity of $10^{37} \text{ erg s}^{-1}$ at 3 kpc. We also tried other deconvolutions of the broad-band spectrum, i.e. Comptonization-emission models (thermal and with bulk motion) or a power-law plus a BB model, but they always yielded unacceptable fits with structured residuals at high energies. We next adopted more complex models for the continuum, as a BMC model modified with a high-energy cut-off. This resulted in a better fit than the single absorbed BMC model, but structured residuals still appear below 10 keV. The best fit is obtained adding a BB model to a BMC modified with a high-energy cut-off (HIGHECUT in XSPEC). A summary of all the spectral parameters reported in Table 6, while the best deconvolution of the broad-band IGR J08408–4503 emission is shown in Fig. 8.

Unlike XTE J1739–302, a cut-off is clearly needed in the spectrum of IGR J08408–4503. Indeed, BMC alone (that is a non-attenuated power law at high energies) does not fit the data well and the multiplicative factor HIGHECUT is needed. We note that the fit clearly points to two distinct photon populations (~ 0.3 and 1.5 – 2 keV), but the current statistics does not allow us to constrain which of the two is seen directly as a BB and which provides part of the seed photons for Comptonization (hence, we include twice the same model in Table 6, one per configuration. See the Section 4 for possible interpretations).

3.4 Timing analysis

We performed a timing analysis on the three sources to investigate for the presence of X-ray pulsations. A Z^2_1 test (Buccheri et al. 1983) on the fundamental harmonics was applied on the events collected in each WT mode sequence (see Table 1) searching in the frequency

range between 0.005 and 100 Hz with a frequency resolution of $1/\Delta T$ Hz, where ΔT is the duration of the WT segment. The resulting power spectrum does not reveal any significant deviations from a statistically flat distribution. Data collected in PC mode were not analysed because of their much lower statistics content.

4 DISCUSSION AND CONCLUSIONS

We report on three new outbursts from three different Supergiant Fast X-ray Transients, XTE J1739–302, IGR J17544–2619 and IGR J08408–4503, observed with *Swift*.

4.1 Spectroscopy

All these three sources were observed in outburst with *Swift* in the past, thus allowing a proper comparison between the spectral properties of the different flares.

For IGR J17544–2619, only the spectrum below 10 keV is available. Compared with the emission previously observed (Paper III), it displays a more absorbed and softer emission (single power-law model). A similar behaviour from IGR J17544–2619 has been recently reported by Rampy, Smith & Negueruela (2009) during a Suzaku observation catching the source during a long outburst (at least three days of accreting phase) in 2008 March (the same reported in Paper III). The XRT/WT spectrum is compatible with spectral parameters reported for the segment n. 6 of the XIS observation (Rampy et al. 2009). A good fit to the IGR J17544–2619 XRT spectrum can also be obtained with a BB model, resulting in a temperature of 1–2 keV, and in a BB radius (at 3.6 kpc) of about 1–1.5 km, compatible with an origin in the neutron star polar cap.

XTE J1739–302 displays for the first time a variable absorption column density within a flare. This behaviour was also observed

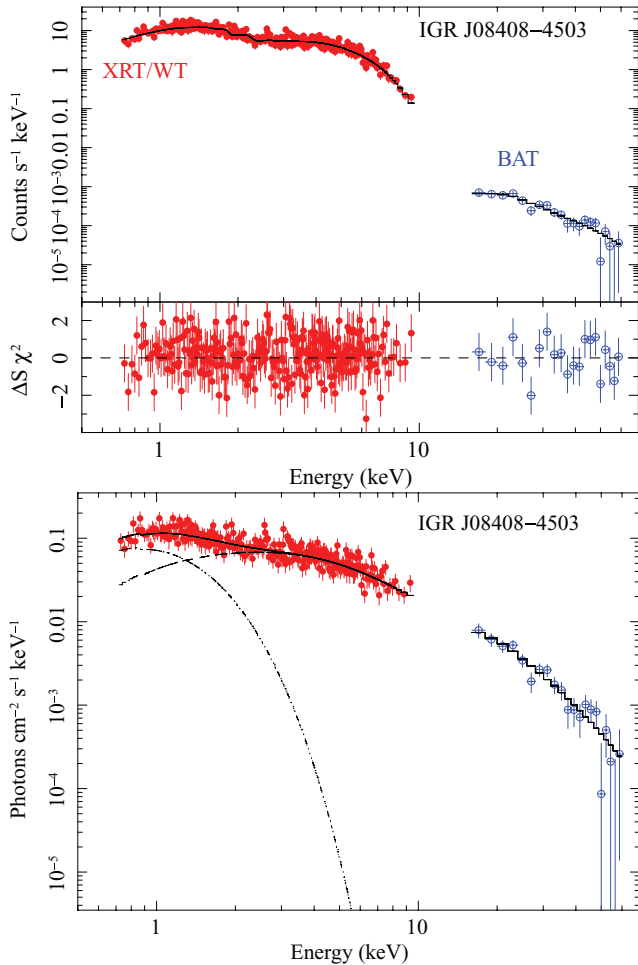


Figure 8. *Swift*/XRT broad-band spectrum (BAT plus simultaneous WT data) of IGR J08408–4503, fitted with a BMC model in *xSPEC* modified with a high-energy cut-off (`HIGHECUT` in *xSPEC*), together with a simple BB at low energies (last model in Table 6 tab:src:spec). The upper panel shows the counts spectrum together with the residuals in units of standard deviations. The lower panel shows the photon spectrum.

in IGR J08408–4503 during the multiple flaring activity caught by *Swift* in 2008 July (Romano et al. 2009a). A higher absorption is observed during the rise to the flare peak, so it is possibly due to the accumulation of matter on to the compact object, instead of obscuring material into the line of sight located far away from the central X-ray source. The average column density is intermediate between the out-of-outburst emission (Paper I) and that displayed during the previous bright flare reported in Paper III. No correlation of the spectral parameters with the source flux can be found. A variability on short time-scales in the obscuring column density of a similar amount was observed also during an outburst from IGR J17544–2619 with *Suzaku* (Rampy et al. 2009). This sudden absorption episode was interpreted as due to the transit of a foreground dense cloud of matter passing in front of the compact object, and as the first direct evidence at X-rays for dense clumps of matter in the supergiant wind. The simultaneous spectroscopy of the XRT and BAT data of XTE J1739–302 can be adequately performed using a simple BMC model (Table 3): a significant fraction ($\log A > 0$) of the initial BB seed photons ($kT_{\text{BB}} \sim 1.6$ keV) is efficiently up-scattered ($\alpha \sim 1.3$) by the Comptonizing plasma. The radius associated with

the BB component of the BMC model is about 1.6 km (at 2.7 kpc), thus consistent with a polar cap origin. The model `COMP`TT allows us to quantify the physical conditions of the Comptonizing plasma, since it returns the plasma temperature kT_e and optical depth τ , instead of the Comptonization efficiency α . As shown in Table 3, the kT_e temperature could not be constrained and this is consistent with the fact that the data could be fitted well by the BMC model that indeed has no cut-off in its spectral shape. These two results point to the fact that the current statistics and data coverage *do not require* a cut-off, although they cannot exclude it. The reason why the `CUT-OFFPL` model fits the data much better than a simple power law resides in the fact that the residuals using a simple power law show an excess around 1–2 keV, whereas the curved shape of the `CUT-OFFPL` linked to the interplay with the absorbing column density can describe the data in a satisfactory way. We note that this excess is naturally taken into account in the physical models, `COMP`TT and BMC, where a 1–2 keV BB seed photon population is obtained. Unfortunately, the current data set does not allow us to investigate the evolution of the high-energy part of the spectrum, so little can be currently said about the possible evolution of the Comptonizing medium. For the remaining part of the outburst, only the softer part below 10 keV is available. Nevertheless, it can be seen from Table 2 that a BB is more suitable to fit the *Swift*/XRT data rather than a power law, consistent with what is obtained in the overall XRT+BAT spectrum.

A comparison of the IGR J08408–4503 broad-band spectrum extracted from the bright flare observed in 2008 September with the ones observed with *Swift* in 2008 July and in 2006 October (Romano et al. 2009a) reveals that the new spectrum is more similar to that observed in 2006 (very low absorption, a hard photon index, and a similar high-energy cut-off at around 10–15 keV). Unlike XTE J1739–302, the spectrum of IGR J08408–4503 could not be fit with a single Comptonization model, two additive components were needed: a BB plus a BMC model (the latter with high-energy cut-off). This could be due to the very low absorption at low energy with respect to the other SFXTs studied here that required an additional component to take into account the softer part of the spectrum. The presence of the cut-off implies that the overall spectrum is the result of thermal Comptonization (the BMC model alone has a non-attenuated power-law shape). The low value of the α parameter obtained ($\alpha < 0.4$, $\Gamma < 1.4$) is typical for saturated Comptonization.

The seed photon temperature for the thermal Comptonization BMC component and the BB temperature could not be linked to the same value in the fitting process and indeed resulted in two clearly different photon populations, a cold one at about 0.3 keV and a hotter one at 1.4–1.8 keV. The current data did not allow us to establish in a solid way, which one of these two populations is seen directly as a BB and which one ends up being seed photons for the thermal Comptonization. As can be seen in Table 6, both scenarios are statistically acceptable. In one case, we obtain a cold (0.3 keV) BB of about $R = 12$ km directly visible (few percent of the total flux), together with a hotter photon population (1.4 keV) thermally Comptonized (the dominant component), part of which is directly visible ($\log A = 0.8$). This could depict a thermal halo around the neutron star [0.3 keV, as in Ferrigno et al. (2009)] together with BB seed photons from the accreting material, part of which is directly visible (e.g. at the column boundaries) and part is thermally Comptonized (from the accreting matter). This scenario is consistent with what was observed for XTE J1739–302 (Table 3) with the thermal cold halo buried in the high column absorption (an order of magnitude higher than for IGR J08408–4503).

In the second case, we obtain a hotter BB (1.9 keV, possibly from the base of the accreting column, $R \sim 1$ km) directly visible, accounting for about 30 per cent of the total flux, together with a colder plasma (0.3 keV) embedded in a thermally Comptonizing medium ($\log A \sim 3$) such as an atmosphere confined by multipolar or crustal components of the magnetic field [e.g. Ferrigno et al. (2009) and references therein].

With the information at hand, we cannot exclude either of these scenarios. The spectra of High Mass X-Ray Binaries (HMXBs) have been generally described by phenomenological models, and this work is one of the few cases where two distinct spectral components linked to two different physical conditions have been observed (see also Ferrigno et al. 2009).

4.2 Search for periodicities

IGR J17544–2619 was previously observed in outburst with *Swift* in two occasions: on 2007 November 8 and 2008 March 31 (Paper III). This implies that the three bright flares are spaced by ~ 144 and ~ 157 d, respectively. We note, however, that in IGR J17544–2619 the flare that occurred on 2008 September 4 was preceded by intense activity in the previous few days during the observations part of the *INTEGRAL* Galactic bulge monitoring program performed on 2008 August 30, reaching a flux of about 50 mCrab (18–40 keV, Romano et al. 2008a). This seems to indicate an outburst phase which began a few days before the BAT trigger, suggesting an outburst duration of several days (an outburst lasting at least 3 d has also been caught with *Suzaku*; Rampy et al. 2009): this could imply a periodic occurrence of the bright flaring activity, every ~ 150 d. If the X-ray bright flares are triggered periodically during the periastron passage in an eccentric binary, the orbital period is probably about 150 d in IGR J17544–2619. This is consistent with previous findings with *INTEGRAL*, where a possible outburst recurrence time-scale of 165 ± 3 d has been suggested (Walter et al. 2006).

From the times of previous IGR J08408–4503 flares, we suggested (Romano et al. 2009a) that a double-periodicity outburst recurrence of ~ 11 and 24 d was present, thus consistent with the picture where the outbursts are triggered when the compact object, along its orbit, crosses twice an inclined second component of an outflowing dense wind, confined along a preferential plane (e.g. the supergiant equator), inclined with respect to the orbital plane. On the other hand, the last flare from IGR J08408–4503 did not occur at the right times predicted by these double periodicities (the nearest outburst was predicted to occur on 2008 September 13, instead of 2008 September 21). This could indicate that either these derived periodicities are actually wrong (and the flaring activity is not periodic but sporadic) or another mechanism is at work when producing this latter kind of outburst: a possible explanation is that, while the previous outbursts were produced when the neutron star crossed twice the denser wind component, this latter outburst was triggered when the neutron star approached the periastron passage, accreting matter from the polar wind, in an eccentric orbit.

The three sources analysed here do not show any evidence for X-ray pulsations (see Section 3.4).

4.3 SFXTs as a class

During the last outburst, a very good sampling of the XTE J1739–302 light curve was possible [the best light curve during an outburst from this source, to date; see Fig. 9(c)]. We can compare the *Swift*/XRT light curve of XTE J1739–302 with the X-ray luminosity predicted by a Bondi–Hoyle accretion on to the neutron

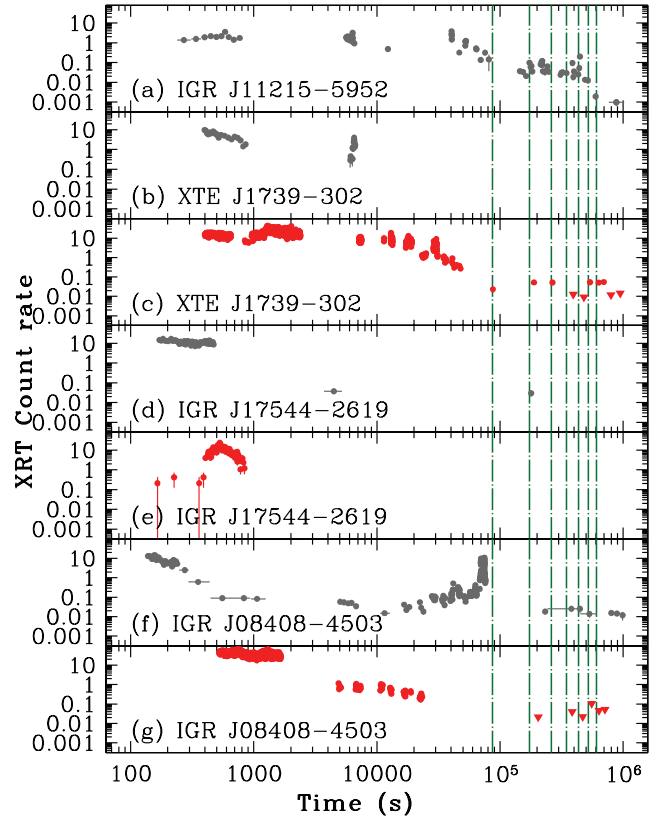


Figure 9. Light curves of the outbursts of SFXTs followed by *Swift*/XRT referred to their respective BAT triggers. Points denote detections and triangles 3σ upper limits. Red data points (panels c, e and g) refer to observations presented here for the first time, while grey data points refer to data presented elsewhere. Note that where no data are plotted, no data were collected. Vertical dashed lines mark time intervals equal to 1 d, up to a week. We show the IGR J11215–5952 light curve (panel a) with an arbitrary start time, since the source did not trigger the BAT (Romano et al. 2007). Panels (b) and (c) report the two flares from XTE J1739–302 observed on 2008 April 8 (Paper III) and on 2008 August 13 (reported here), respectively. Panels (d) and (e) show the outbursts of IGR J17544–2619 which occurred on 2008 March 31 (Paper III) and the latest one reported here (this outburst, as in IGR J11215–5952, did not trigger the BAT, thus the start time is arbitrary and was set at the beginning of the observation). Panels (f) and (g) show the last two outbursts from another SFXT, not part of the XRT campaign, IGR J08408–4503, which occurred on 2008 July 5 (Romano et al. 2009a) and on 2008 September 21 (reported in this paper).

star from a spherically symmetric homogeneous wind for different values of the orbital period and eccentricity. We assume for the supergiant a stellar mass of $33 M_{\odot}$, a radius of $23 R_{\odot}$ (Vacca, Garmany & Shull 1996), a beta-law for the supergiant wind with $\beta = 1$, a wind terminal velocity of 1900 km s^{-1} , a wind mass loss rate of $10^{-6} M_{\odot} \text{ yr}^{-1}$ and a temperature of the stellar wind of 10^5 K . We find that for any choice of the orbital period and eccentricity the decline of the light curve observed with *Swift* is too rapid compared with the calculated light curve, even adopting high values for the orbital period and eccentricity. Since a spherical distribution of wind matter is not able to explain the observed shape of the X-ray light curve, a possible explanation is the presence of a second outflowing wind component, denser than the supergiant polar wind, which is crossed by the neutron star along its orbit, in analogy to what we proposed for IGR J11215–5952 (Sidoli et al. 2007). Alternatively, if we consider the clumpy wind scenario, from the duration of the

bright part of the flare in XTE J1739–302 (>0.6 d) and its luminosity ($\sim 10^{36}$ erg s^{-1}), we can derive an accreted mass of $>4 \times 10^{25}$ g and a size of $>10^{13}$ cm (Walter & Zurita Heras 2007), which corresponds to more than six supergiant radii, thus making very unlikely that it is a very large single clump ejected by the supergiant (Walter & Zurita Heras 2007). Instead, it could be alternatively explained with a huge gas stream composed by several smaller clumps.

In Fig. 9, we compare some of the outbursts from SFXTs as observed during our monitoring campaign. In particular, the three outbursts discussed here are shown in panels c, e and g from XTE J1739–302, IGR J17544–2619 and IGR J08408–4503, respectively. One could be tempted to conclude, from this comparison, that different types of outburst are present, even in the same source. It is actually not possible to compare, for example, the two outbursts from IGR J08408–4503 (last panels in Fig. 9): the several upper limits to the flux in the declining part of the outbursts are compatible with the source detections during the previous IGR J08408–4503 outburst [Fig. 9(f)], thus it is not possible to conclude that the new outburst from IGR J08408–4503 [Fig. 9(g)] is shorter than the previous one [Fig. 9(f)]. On the other hand, the light curve from XTE J1739–302 [Fig. 9(c)] allows us to perform a proper comparison with the outburst from the periodic SFXTs IGR J11215–5952 [Fig. 9(a); Sidoli, Paizis & Mereghetti 2006; Romano et al. 2007]: these two sources appear to undergo similar outbursts with a similar duration. Interestingly, Rampy et al. (2009) report on a long outburst activity from IGR J17544–2619 during the 2008 March outburst, with a rise time much longer than what observed with *Chandra* during an X-ray flare in 2004 (in't Zand 2005) in the same source. These authors suggest that different kinds of outbursts can occur in the same SFXT.

From the duration of single well-sampled short flares in IGR J08408–4503, we derived an orbital period of about 35 d (Romano et al. 2009a) adopting an expansion law for the clump sizes as the clump is accelerated far away from the supergiant donor, in the framework of an inhomogeneous wind (Romano et al. 2009a). Adopting this same expansion law, and from the observed durations of the short flares which compose the outburst light curves in XTE J1739–302 and IGR J17544–2619, we can derive the distance of the accreted clump from the supergiant star, as we did in IGR J08408–4503 (Romano et al. 2009a). More details will be reported in Ducci et al. (2009). Fitting with a Gaussian a few well-sampled flares in XTE J1739–302, we obtain a full width at half-maximum (FWHM) of 260 ± 60 and 390 ± 60 s, while in IGR J17544–2619 the observed flare has a duration of 220 ± 10 s (FWHM). From the clump expansion law reported in Romano et al. (2009a), we derive a distance of the compact object from the supergiant donor in these two sources as follows: in the range from 6.8×10^{12} to 1.25×10^{13} cm for XTE J1739–302, while near to 6.8×10^{12} cm for IGR J17544–2619 (assuming a supergiant mass of $33 M_{\odot}$ and a stellar radius of $23 R_{\odot}$). Assuming a circular orbit, these distances translate into orbital periods ranging from 20 to 50 d in XTE J1739–302 and around 20 d for IGR J17544–2619. This latter orbital period is not consistent with that of ~ 150 d, suggested by the outburst recurrence in IGR J17544–2619. This discrepancy can be easily reconciled if the orbit in this SFXT is highly eccentric.

Jain, Paul & Dutta (2009) recently reported on the discovery of an orbital period of 3.3 d from the SFXT IGR J16479–4514. This orbital periodicity is even shorter than that displayed by several persistent HMXBs with supergiant companions. This poses serious problems to the different physical mechanisms proposed for SFXTs, implying an orbital separation of about 2×10^{12} cm (assuming a su-

pergiant mass of $\sim 30 M_{\odot}$), which is about 1.2 stellar radii, thus well inside the region where the highest wind clump number density is expected, and a persistent X-ray emission is predicted (Negueruela et al. 2008). The very different orbital periods discovered in SFXTs to date (ranging from 3.3 to 165 d) possibly point to different kinds of SFXTs (different mechanisms at work in different sources, and possibly in the same source, as discussed above).

ACKNOWLEDGMENTS

LS thanks INAF-IASF Palermo and PR thanks INAF-IASF Milano, where some of the work was carried out, for their kind hospitality. We thank Valentina La Parola and Cristiano Guidorzi for helpful discussions. We thank the *Swift* team for making these observations possible, the duty scientists, and science planners. This work was supported in Italy by ASI contracts I/023/05/0, I/088/06/0 and I/008/07/0, and partially by the grant from PRIN-INAF 2007, ‘Bulk motion Comptonization models in X-ray Binaries: from phenomenology to physics’ (PI M. Cocchi). HAK was supported by the *Swift* project. DNB and JAK acknowledge support from NASA contract NAS5-00136.

REFERENCES

- Bamba A., Yokogawa J., Ueno M., Koyama K., Yamauchi S., 2001, PASJ, 53, 1179
- Bird A. J., Malizia A., Bazzano A., Barlow E. J., Bassani L., Hill A. B., 2007, ApJS, 170, 175
- Blay P. et al., 2008, A&A, 489, 669
- Buccheri R. et al., 1983, A&A, 128, 245
- Burrows D. N. et al., 2005, Space Sci. Rev., 120, 165
- Ducci L., Sidoli L., Paizis A., Mereghetti S., 2008, preprint (arXiv:0810.5963)
- Ducci L., Sidoli L., Mereghetti S., Paizis A., Romano P., 2009, MNRAS, submitted
- Ferrigno C., Becker P. A., Segreto A., Mineo T., Santangelo A., 2009, A&A, 498, 825
- Götz D., Schanne S., Rodriguez J., Leyder J.-C., von Kienlin A., Mowlavi N., Mereghetti S., 2006, Astron. Tel., 813, 1
- Götz D., Falanga M., Senziani F., De Luca A., Schanne S., von Kienlin A., 2007, ApJ, 655, L101
- Grebenev S. A., Lutovinov A. A., Sunyaev R. A., 2003, Astron. Tel., 192
- Grebenev S. A., Rodriguez J., Westergaard N. J., Sunyaev R. A., Oosterbroek T., 2004, Astron. Tel., 252
- in't Zand J. J. M., 2005, A&A, 441, L1
- Jain C., Paul B., Dutta A., 2009, preprint (arXiv:0903.5403)
- Kennea J. A., Campana S., 2006, Astron. Tel., 818, 1
- Krimm H. A. et al., 2007, Astron. Tel., 1265, 1
- Kuulkers E. et al., 2007, Astron. Tel., 1266, 1
- Mangano V. et al., 2008, Astron. Tel., 1727, 1
- Masetti N., Bassani L., Bazzano A., Dean A. J., Stephen J. B., Walter R., 2006a, Astron. Tel., 815, 1
- Masetti N. et al., 2006b, A&A, 449, 1139
- Mereghetti S., Sidoli L., Paizis A., Gotz D., 2006, Astron. Tel., 814, 1
- Negueruela I., Smith D. M., Harrison T. E., Torrejón J. M., 2006, ApJ, 638, 982
- Negueruela I., Torrejón J. M., Reig P., Ribo M., Smith D. M., 2008, in Bandyopadhyay R. M., Wachter S., Gelino D., Gelino C. R., eds, AIP Conf. Proc. Vol. 1010, A Population Explosion: The Nature & Evolution of X-Ray Binaries in Diverse Environments. Am. Inst. Phys., New York, p. 252
- Pellizza L. J., Chaty S., Negueruela I., 2006, A&A, 455, 653
- Rahoui F., Chaty S., Lagage P.-O., Pantin E., 2008, A&A, 484, 801
- Rampy R. A., Smith D. M., Negueruela I., 2009, preprint (arXiv:0904.1189)
- Romano P., Sidoli L., Mangano V., Mereghetti S., Cusumano G., 2007, A&A, 469, L5

- Romano P. et al., 2008a, *Astron. Tel.*, 1697
Romano P. et al., 2008b, *Astron. Tel.*, 1659
Romano P. et al., 2008c, *ApJ*, 680, L137 (Paper II)
Romano P. et al., 2009a, *MNRAS*, 392, 45
Romano P. et al., 2009b, *Astron. Tel.*, 1920, 1
Sakano M., Koyama K., Murakami H., Maeda Y., Yamauchi S., 2002, *ApJS*, 138, 19
Sguera V. et al., 2005, *A&A*, 444, 221
Sguera V. et al., 2006, *ApJ*, 646, 452
Sidoli L., 2009, *Adv. Space Res.*, 43, 1464
Sidoli L., Paizis A., Mereghetti S., 2006, *A&A*, 450, L9
Sidoli L., Romano P., Mereghetti S., Paizis A., Vercellone S., Mangano V., Götz D., 2007, *A&A*, 476, 1307
Sidoli L. et al., 2008a, *Astron. Tel.*, 1454, 1
Sidoli L. et al., 2008b, *ApJ*, 687, 1230 (Paper I)
Sidoli L. et al., 2009, *ApJ*, 690, 120 (Paper III)
Smith D. M., Main D., Marshall F., Swank J., Heindl W. A., Leventhal M., in 't Zand J. J. M., Heise J., 1998, *ApJ*, 501, L181
Sunyaev R. A., Grebenev S. A., Lutovinov A. A., Rodriguez J., Mereghetti S., Gotz D., Courvoisier T., 2003, *Astron. Tel.*, 190
Titarchuk L., 1994, *ApJ*, 434, 570
Titarchuk L., Mastichiadis A., Kylafis N. D., 1996, *A&AS*, 120, C171
Vacca W. D., Garmany C. D., Shull J. M., 1996, *ApJ*, 460, 914
Vaughan S. et al., 2006, *ApJ*, 638, 920
Walter R. et al., 2006, *A&A*, 453, 133
Walter R., Zurita Heras J., 2007, *A&A*, 476, 335

This paper has been typeset from a $\text{\TeX}/\text{\LaTeX}$ file prepared by the author.